Transactions of the TSME (2018) Vol. 6, No. 2, 113-130
Journal of Research and Applications in Mechanical Engineering

ISSN 2229-2152 print
DOI: 10.14456/jrame.2018.11

Research Article

THE EFFECT OF STATIC AND DYNAMIC LOADING ON FEMORAL BONE USING FINITE ELEMENT ANALYSIS

K. Chalernphon[1]
P. Aroonjarattham[2,*]
K. Aroonjarattham[3]
C. Somtua[2]
[1] Galaxi Laboratory, Geo-Informatics and Space Technology Development Agency (GISTDA), 88 Moo 9 Tambon Thung Sukala, Amphoe Siracha, Chonburi 20230, Thailand
[2] Department of Mechanical Engineering, Faculty of Engineering, Mahidol University, 25/25, Phuttamonthol Sai 4 Rd., Salaya, Phuttamonthol, Nakornpathom 73170, Thailand
[3] Department of Orthopaedics, Faculty of Medicine, Burapha University, 169 Long-Had Bangsaen Rd., Muang District, Chonburi 20131 Thailand

ABSTRACT:
In using finite element analysis on bone-implant models, the static loading condition is the peak load of dynamic loading condition under daily activities. Dynamic loading will affect the strain distribution on the bone and stress distribution on the implant. In this research, the normal bone, bone inserted with load-bearing device and bone inserted with load-sharing device under static and dynamic loading conditions were analyzed to compare the stress distribution on the implant and strain distribution on the bone. The results show that the maximum difference of equivalent total strain between static loading condition and dynamic loading condition in normal bone is less than 20%, in bone inserted load-bearing device is less than 12%, and in bone inserted load-bearing device is less than 30%. The maximum difference of von Mises stress between static loading condition and dynamic loading condition in load-bearing device is less than 3% but exceeds 105% for load-sharing device. The static loading and dynamic loading conditions can be used interchangeably in analyzing normal bone and load-bearing devices while dynamic loading condition is considered more suitable for load-sharing devices in finite element analysis of bone-implant models.

Keywords: *Dynamic loading, static loading, femoral bone, finite element analysis*

1. INTRODUCTION

Finite element analysis had been widely used to evaluate the stress and strain distribution on bone-implant model under static loading [1-4]. The boundary conditions were derived from Heller *et al*., (2004) by using the peak load during the human activity as walking and stair-climbing condition [5] but the dynamic loading was similarly to the daily activities than the static loading, was act as the continuous load. Dynamic loading will be affected the strain distribution on the bone and stress distribution on the implant because the muscular force and body weight act on proximal femur was varied with time under dynamic loading then the implant did not receive the peak load all the time as static loading.

Femur was a largest, longest and strongest bone of a human body that carried the body weight and absorbed the shock load during daily activities. When the femur was damaged, the operative surgery was the most successful method to help the patient return to the normal life. Implant used to insert the femur was divided two types [6] as load-bearing device [7, 8] and load-sharing device [9].

* Corresponding author: P. Aroonjarattham
E-mail address: panya.aro@mahidol.ac.th

This research aimed to use the finite element analysis to evaluate the stress distribution on two different types of implants: load-bearing devices as hip prosthesis and load-sharing devices as intramedullary nail respectively; and strain distribution on the femoral bone under dynamic loading condition, in order to compare with the results from static loading counterpart. The result from this study can help decide which loading condition is suitable to be used to analyze which type of implants.

2. MATERIALS AND METHODS

2.1 Femoral bone model

Three-dimensional model of femoral bone was scanned by the computed tomography (CT) scanner and was reconstructed by ITK-SNAP program [2]. The model was divided into four main parts as proximal cortex, proximal cancellous, distal cortex and distal cancellous as shown in Fig. 1.

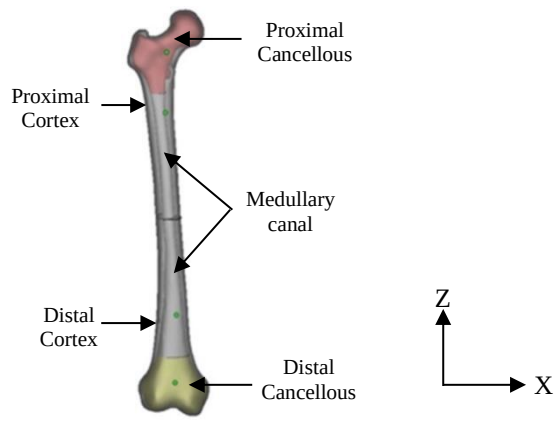

Fig. 1. Three-dimensional model of femoral bone.

2.2 Hip prosthesis model

The cementless hip prosthesis was used in this study because of the low rates of aseptic, loosening and stability for the bone ingrowth [10-13]. The model of hip prosthesis was created from SolidWorks CAD software by measuring the actual hip prosthesis as shown in Fig. 2.

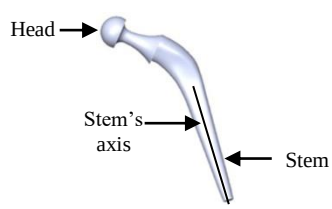

Fig. 2. Three-dimensional model of hip prosthesis.

2.3 Intramedullary nail model

The intramedullary nail was created from SolidWorks CAD software that had a nail axis 1,500 mm and thickness 1.2 mm. The screw was assumed as a cylindrical shape because the nail and core diameter had more effect than the thread profile. The model of intramedullary nail and four screws was shown in Fig. 3.

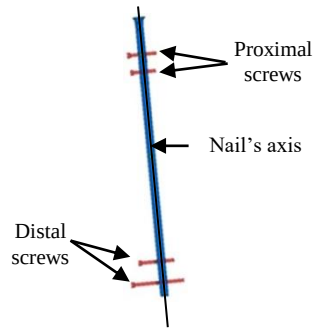

Fig. 3. Three-dimensional model of intramedullary nail and four screws.

2.4 Virtual simulation

Virtual simulation technique was used to insert the hip prosthesis and intramedullary nail to the femur with the actual surgery position.

2.4.1 Hip prosthesis

Hip prosthesis was inserted into the femur, which was removed of the femoral head. The hip stem axis was placed in perfect alignment with the medullary canal's axis and fit with the hollow of the femur as shown in Fig. 4.

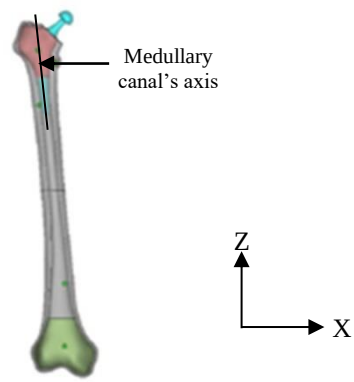

Fig. 4. Femoral bone inserted hip prosthesis.

2.4.2 Intramedullary nail

The nail's axis and medullary canal's axis were in alignment with the best fit position as shown in Fig. 5. The bone model was assigned to fracture at the mid-shaft of the bone [14]. The fracture type was comminuted fracture by the fracture fragment with 5 mm. in length. The mid-shaft of femur was assumed as the fracture gap and replaced by connective tissue to simulate healing status.

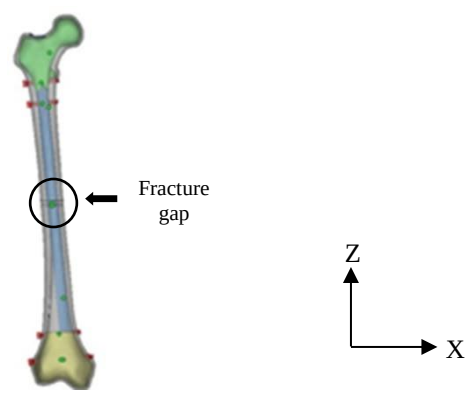

Fig. 5. Femoral bone with fracture gap at mid-shaft inserted intramedullary nail.

2.5 Case analysis

All models were analyzed to evaluate the maximum equivalent of total strain on the bone and the maximum von Mises stress on the implant under daily activities as walking and stair-climbing conditions. The case analysis was divided to three cases as normal bone, femur inserted with hip prosthesis and femur inserted with intramedullary nail. The dynamic condition had varied time duration as 1, 0.5, 0.1, 0.05 and 0.01 second refers to normal and accidental gait cycles. All cases analysis was shown in Table 1.

Table 1: List of condition in the analysis.

Cases	Model	Loading condition	Time (sec)
1	Normal bone	Static	1
2	Normal bone	Dynamic	1, 0.5, 0.1, 0.05, 0.01
3	Femur inserted with hip prosthesis	Static	1
4	Femur inserted with hip prosthesis	Dynamic	1, 0.5, 0.1, 0.05, 0.01
5	Femur inserted with intramedullary nail	Static	1
6	Femur inserted with intramedullary nail	Dynamic	1, 0.5, 0.1, 0.05, 0.01

2.6 Contact condition

MSC software was defined the relationship of the part contact as no contact, touch contact and glue contact condition. The touch contact condition was applied to the intramedullary nail contact the femoral shaft that was assumed the implant had movement in the medullary canal. The glue contact condition was applied to the hip prosthesis contact the bone cut and the screw fixation contact the femoral bone that was assumed to simulate an implant rigidly fixed result of the bone ingrowths [15].

2.7 Boundary condition

The boundary condition used in this research was a daily activities load that measured by Electromyography (EMG). EMG was a technique to evaluate and record the electrical activity produced by skeletal muscle [16]. The body weight act on the femoral head and the muscular force act on the proximal part under walking and stair-climbing conditions. This research was divided two subjects main as static loading and dynamic loading by preparation as follows:

2.7.1 Static loading condition

The magnitude of muscular forces was shown in Table 2 for walking and stair-climbing condition. Static loading was used the peak load from the gait cycle to analyze.

Table 2: The load condition which applied to femoral bone [5].

Position	Force	Walking			Stair-climbing		
		F_x (N)	F_y (N)	F_z (N)	F_x (N)	F_y (N)	F_z (N)
1	Fix displacement	0	0	0	0	0	0
2	Body weight	0	0	-836.0	0	0	-847.0
3	Hip contact	-54.0	-32.8	-229.2	-59.3	-60.6	-236.3
4	Intersegmental resultant	-8.1	-12.8	-78.2	-13.0	-28.0	-70.1
5	Abductor	58.0	4.3	86.5	70.1	28.0	84.9
6	Ilio-tibial tract, proximal part	0	0	0	10.5	3.0	12.8
7	Ilio-tibial tract, distal part	0	0	0	-0.5	-0.8	-16.8
8	Tensor fascia latae, proximal part	7.2	11.6	13.2	3.1	4.9	2.9
9	Tensor fascia latae, distal part	-0.5	-0.7	-19.0	-0.2	-0.3	-6.5
10	Vastus lateralis	-0.9	18.5	-92.9	-2.2	22.4	-135.1
11	Vastus medialis	0	0	0	-8.8	39.6	-267.1

2.7.2 Dynamic loading condition

The dynamic loading condition was analyzed the hip contact force and the muscular force varied with time during the entire load cycle. The dynamic walking was shown the hip contact force and the muscular force in Fig. 6 and the dynamic stair-climbing was shown the hip contact force and the muscular force in Fig. 7 [16].

The positions of hip contact and muscular forces for daily activities were operated on the proximal femur as shown in Fig. 8.

2.8 Material properties

All material properties were assumed to be homogeneous, isotropic and linear elastic. Material properties of cortical bone, cancellous bone, initial connective tissue, titanium alloy (hip prosthesis) and stainless steel (intramedullary nail) were shown in Table 3.

Table 3: Material properties of all models [17, 18].

Material	Young's modulus (MPa)	Poisson's ratio
Cortical bone	14,000	0.3
Cancellous bone	600	0.2
Initial connective tissue	3	0.4
Titanium alloy	110,000	0.3
Stainless steel (AISI 316L)	200,000	0.3

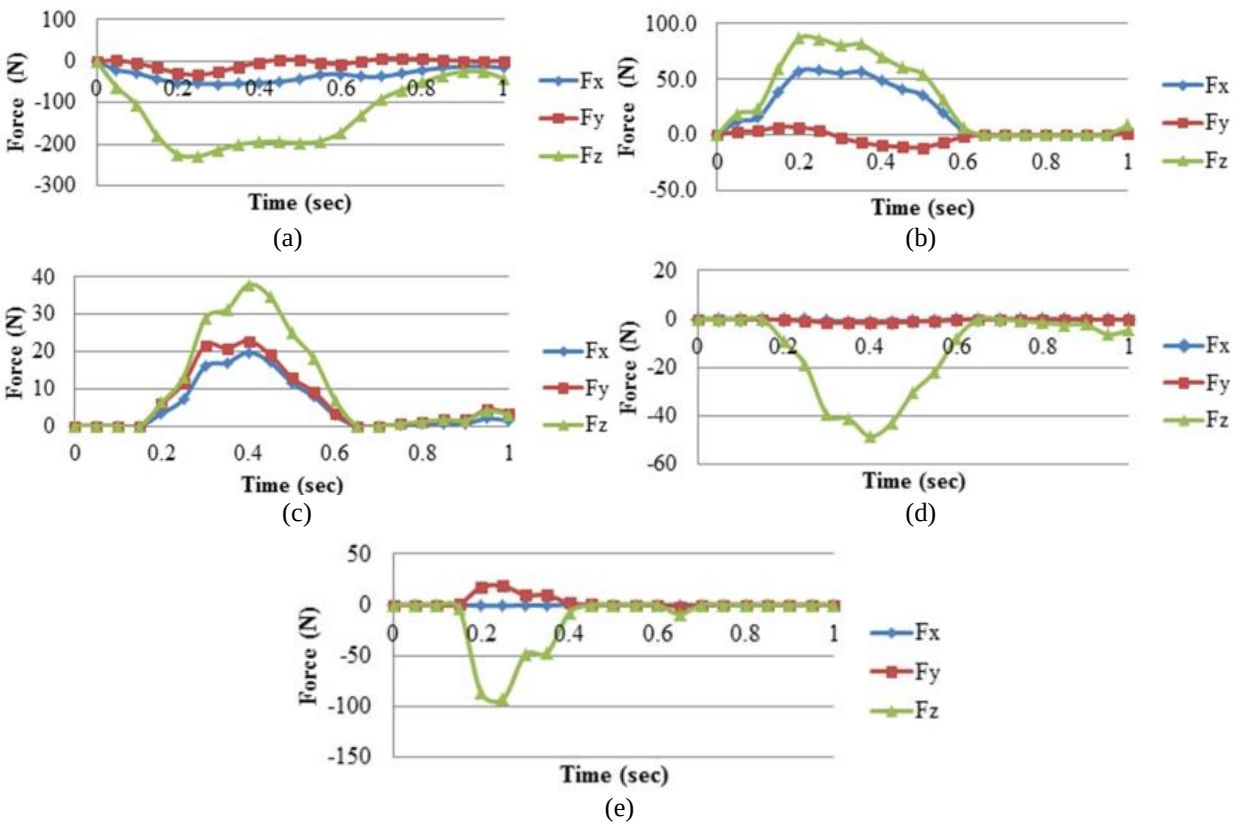

Fig. 6. The force varied with time under dynamic walking condition: (a) Hip contact force, (b) Abductor, (c) Tensor fascia latae, proximal part, (d) Tensor fascia latae, distal part and (e) Vastus lateralis.

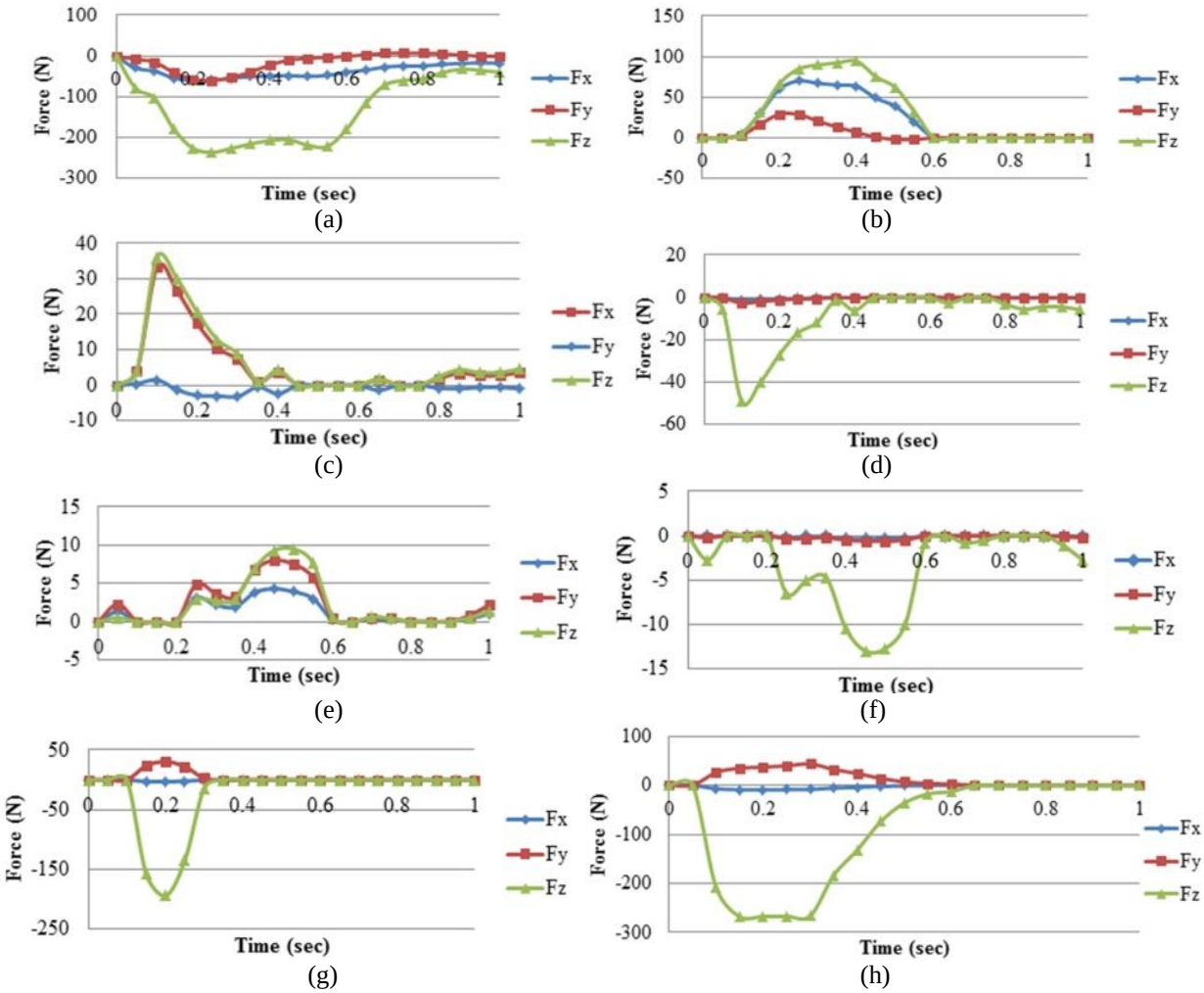

Fig. 7. The force varied with time under dynamic stair-climbing condition: (a) Hip contact force, (b) Abductor, (c) Ilio-tibial tract, proximal part, (d) Ilio-tibial tract, distal part, (e) Tensor fascia latae, proximal part, (f) Tensor fascia latae, distal part, (g) Vastus lateralis and (h) Vastus medialis.

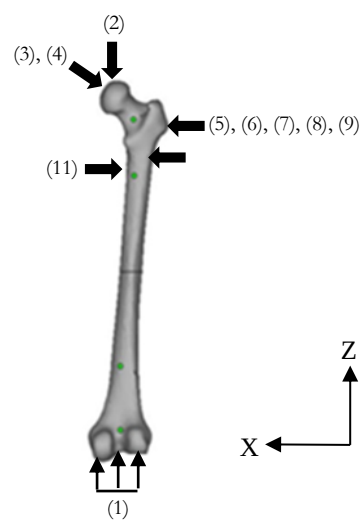

(1) Fix displacement
(2) Body weight
(3) Hip contact
(4) Intersegmental resultant
(5) Abductor
(6) Ilio-tibial tract, proximal part
(7) Ilio-tibial tract, distal part
(8) Tensor fascia latae, proximal part
(9) Tensor fascia latae, distal part
(10) Vastus lateralis
(11) Vastus medialis

Fig. 8. The position of loading on femoral bone.

2.9 Mesh generation

All models were generated mesh model with four-node tetrahedral element by the MSC software package [19]. Femoral bone had a total of 58,429 nodes and 239,474 elements. Femur inserted hip prosthesis had a total of 57,155 nodes and 233,341 elements. Femur inserted intramedullary nail had a total of 135,685 nodes and 525,454 elements. Mesh models of proximal part were shown in Fig. 9.

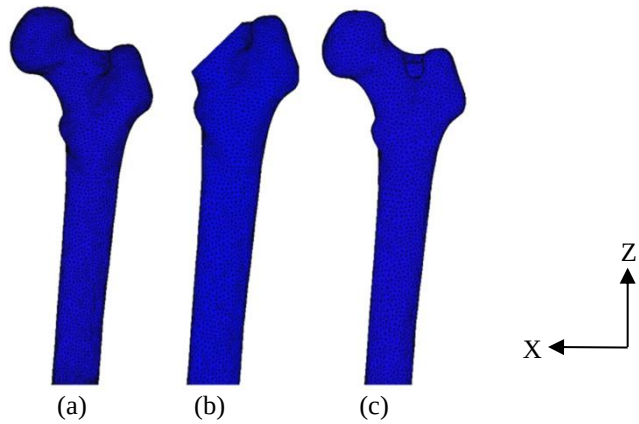

Fig. 9. Mesh model of proximal part: (a) Femoral bone, (b) Femur inserted hip prosthesis and (c) Femur inserted intramedullary nail.

All mesh models were tested to find the optimal mesh size by convergent test, was tested for find the minimum mesh sizes that give the exact solution and use less calculation time. It was varied the mesh size between 0.6, 0.7, 0.8, 1, 1.5 and 2 millimetres. The result of convergent test was shown in Fig. 10 and the mesh size of 0.8 millimetres was used in this study.

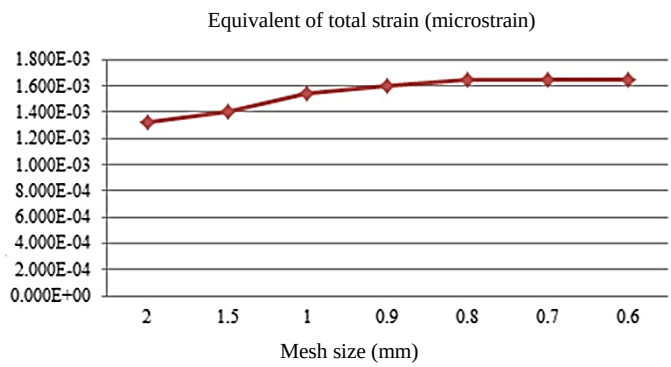

Fig. 10. The convergent test between mesh size and equivalent of total strain.

3. RESULTS AND DISCUSSION

All models were evaluated by FEA under static and dynamic loading conditions to obtain the von Mises stress on the implant and the equivalent of total strain distribution on the bone model.

3.1 Normal bone

The normal bone was analyzed under four load cases as static walking, dynamic walking, static stair-climbing and dynamic stair-climbing. The results of equivalent of total strain distribution on the bone under static and dynamic walking were shown in Fig. 11 and under static and dynamic stair-climbing were shown in Fig. 12 respectively.

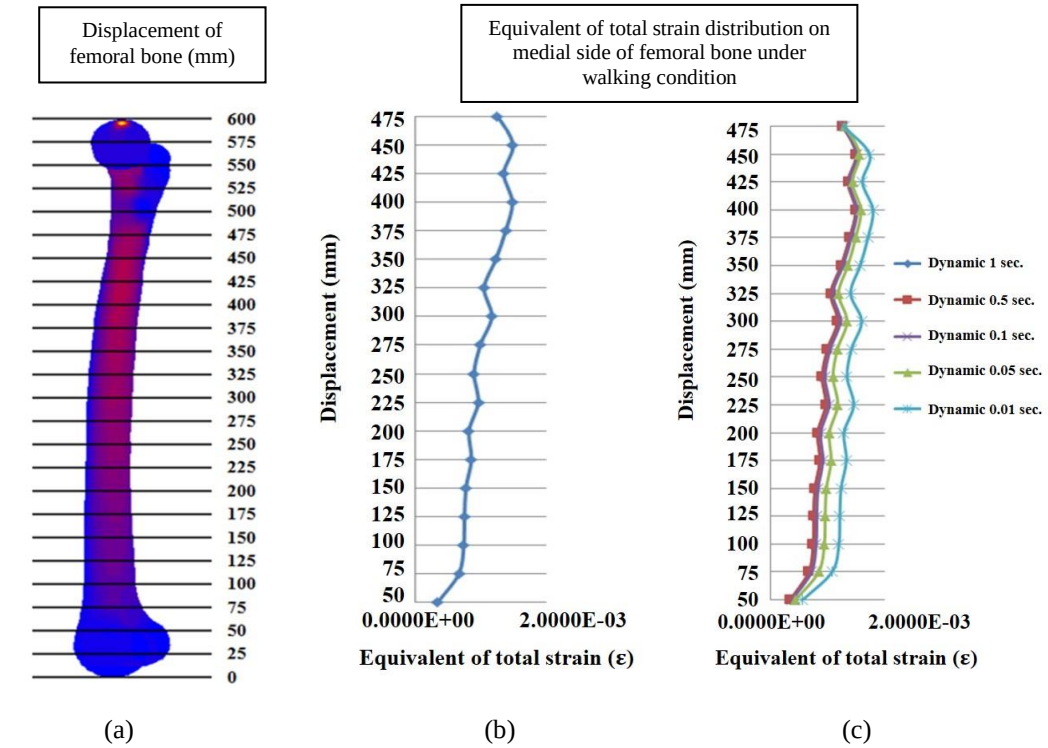

Fig. 11. Equivalent of total strain distribution at medial side of femoral bone: (a) Normal bone, (b) Static loading condition and (c) Dynamic loading condition.

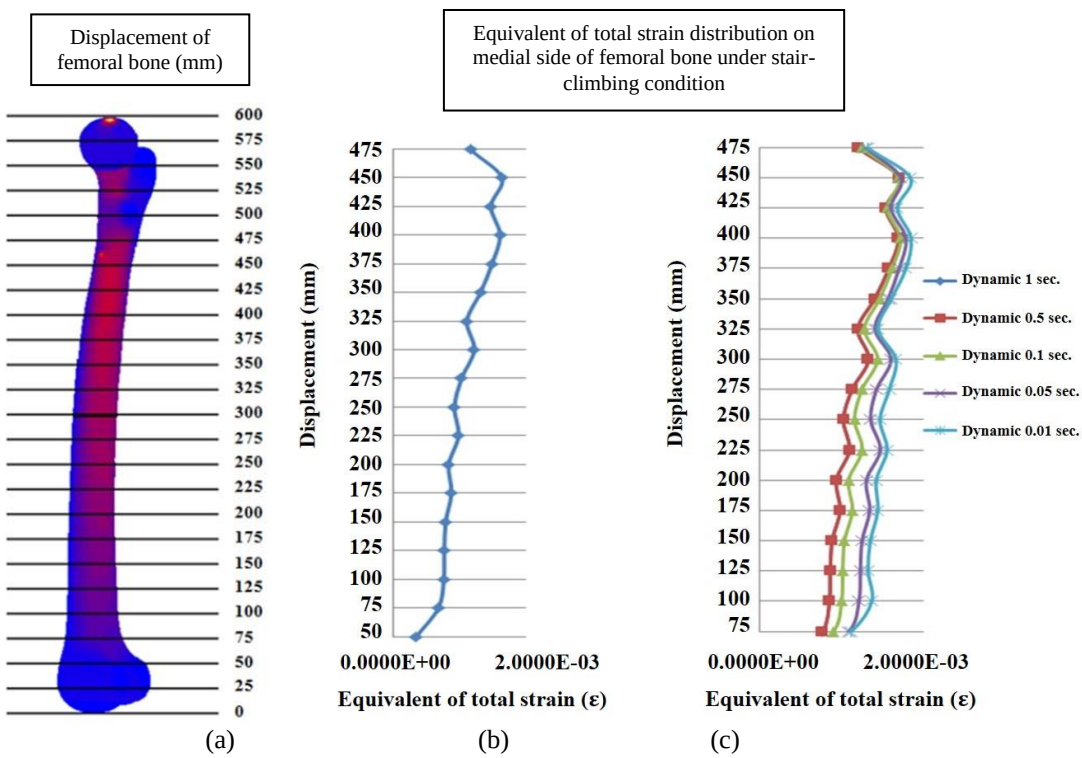

Fig. 12. Equivalent of total strain distribution at medial side of femoral bone: (a) Normal bone, (b) Static loading condition and (c) Dynamic loading condition.

The femoral bone was broken when the maximum equivalent of total strain on the bone equal or higher than 25,000 microstrain (με) [20, 21]. All models showed that the maximum equivalent of total strain on femoral bone is less than 25,000 με; and the trend of the maximum equivalent of total strain distribution when varied time under dynamic loading was shown in Fig. 13 and 14 under walking and stair-climbing respectively.

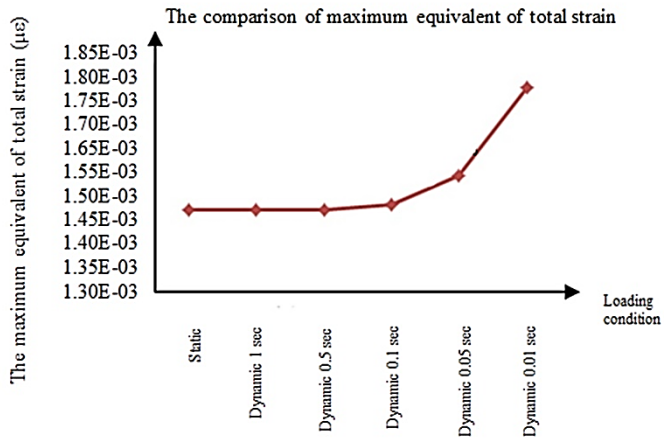

Fig. 13. The comparison of the maximum equivalent of total strain on femoral bone at the medial side under static walking and dynamic walking varied time condition.

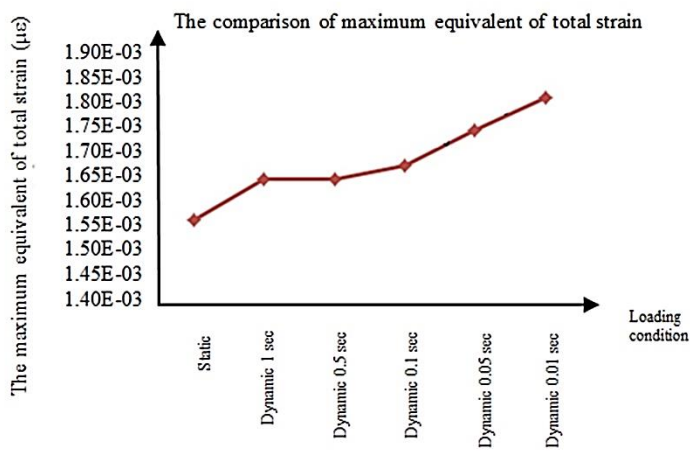

Fig. 14. The comparison of the maximum equivalent of total strain on femoral bone at the medial side under static stair-climbing and dynamic stair-climbing varied time condition.

The comparison of maximum equivalent of total strain on femoral bone between static and dynamic condition had 0% difference in case of 1 sec gait cycle, 0.01% in case of 0.5 sec gait cycle, 0.96% in case of 0.1 sec gait cycle, 5.52% in case of 0.05 sec gait cycle and 19.70% in case of 0.01 sec gait cycle under walking condition and 4.74% in case of 1 sec gait cycle, 4.74% in case of 0.5 sec gait cycle, 6.36% in case of 0.1 sec gait cycle, 10.52% in case of 0.05 sec gait cycle and 14.52% in case of 0.01 sec gait cycle under stair-climbing condition. When the time of gait cycle decreased, the maximum strain distribution on the bone increased; it showed that the strain distribution varies inversely with time of gait cycle.

3.2 Femoral bone inserted with hip prosthesis

Femoral bone inserted with hip prosthesis was analyzed under four load cases as static walking, dynamic walking, static stair-climbing and dynamic stair-climbing. The results of equivalent of total strain distribution on the bone under static and dynamic walking were shown in Fig. 15 and under static and dynamic stair-climbing were shown in Fig. 16 respectively.

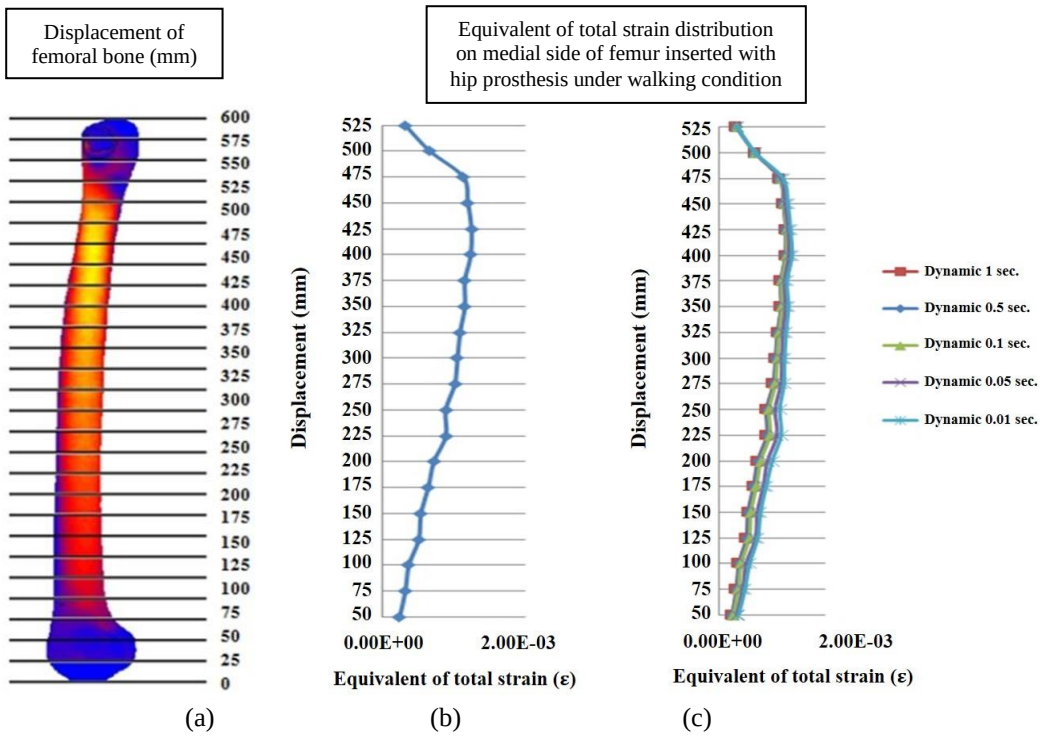

Fig. 15. Equivalent of total strain distribution at medial side of femur inserted with hip prosthesis: (a) Femoral bone, (b) Static loading condition and (c) Dynamic loading condition.

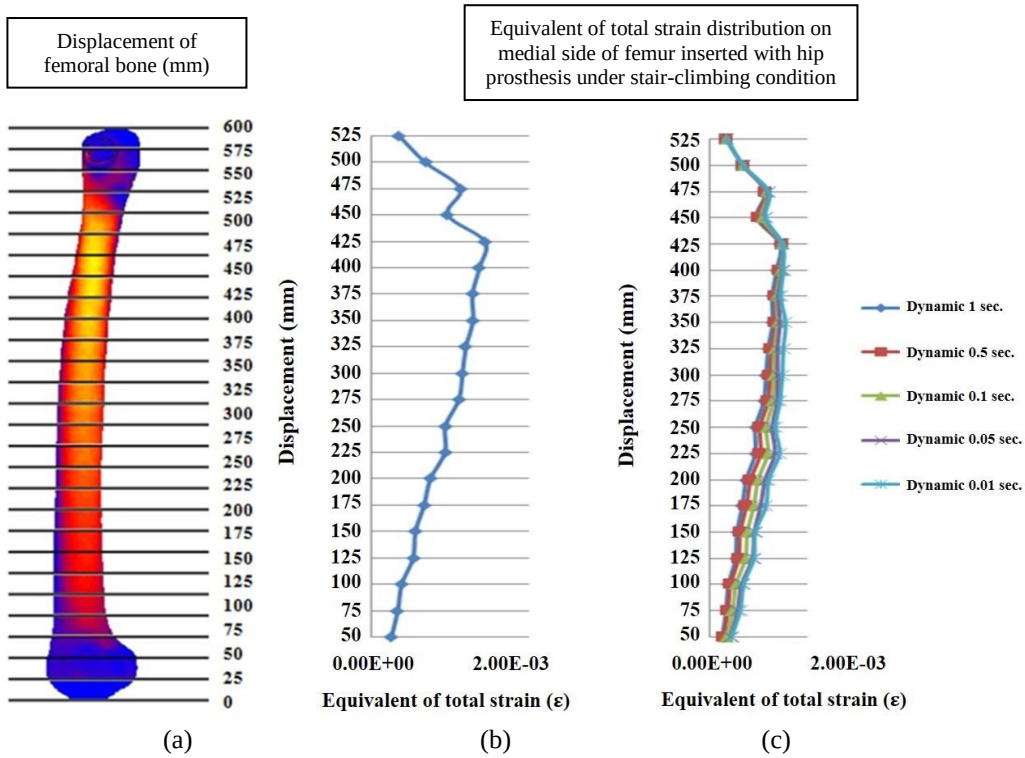

Fig. 16. Equivalent of total strain distribution at medial side of femur inserted with hip prosthesis: (a) Femoral bone, (b) Static loading condition and (c) Dynamic loading condition.

The maximum equivalent of total strain on femoral bone of all models did not exceed 25,000 με; and the trend of the maximum equivalent of total strain distribution when varied time under dynamic loading was shown in Fig. 17 and 18 under walking and stair-climbing respectively.

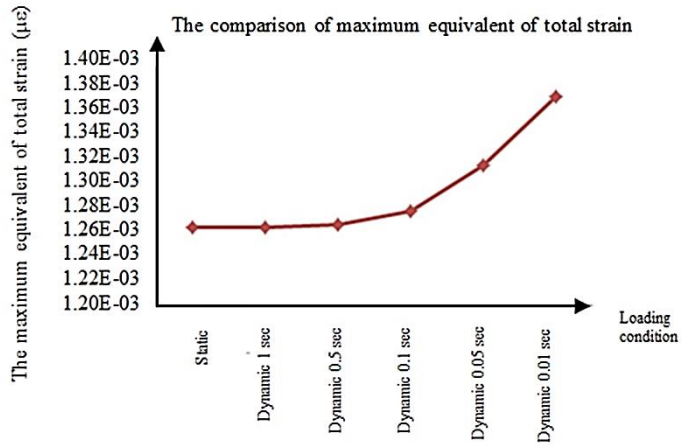

Fig. 17. The comparison of the maximum equivalent of total strain on femur inserted with hip prosthesis at the medial side under static walking and dynamic walking varied time condition.

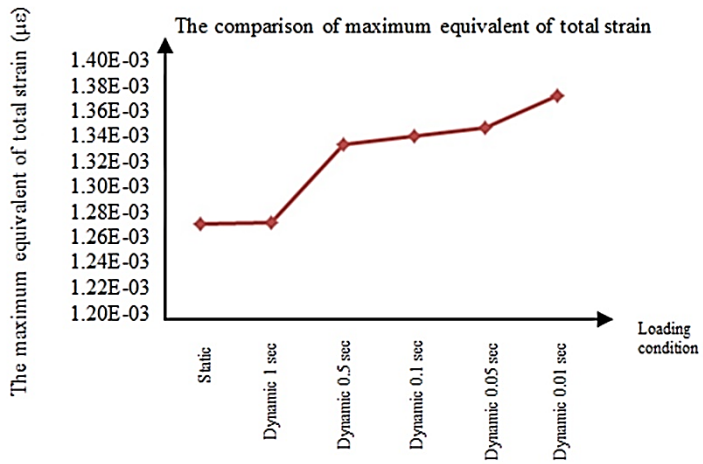

Fig. 18. The comparison of the maximum equivalent of total strain on femur inserted with hip prosthesis at the medial side under static stair-climbing and dynamic stair-climbing varied time condition.

The comparison of maximum equivalent of total strain on femoral bone between static and dynamic conditions had 0.02% difference in case of 1 sec gait cycle, 0.18% in case of 0.5 sec gait cycle, 1.13% in case of 0.1 sec gait cycle, 9.36% in case of 0.05 sec gait cycle and 11.15% in case of 0.01 sec gait cycle under walking condition and 0.01% in case of 1 sec gait cycle, 3.16% in case of 0.5 sec gait cycle, 3.50% in case of 0.1 sec gait cycle, 3.79% in case of 0.05 sec gait cycle and 5.10% in case of 0.01 sec gait cycle under stair-climbing condition. When the time of gait cycle decreased, the maximum strain distribution on the bone increased, it showed that the strain distribution varies inversely with time of gait cycle.

3.3 Femoral bone inserted with intramedullary nail

Femoral bone inserted with intramedullary nail was analyzed under four load cases as static walking, dynamic walking, static stair-climbing and dynamic stair-climbing. The results of equivalent of total strain distribution on the bone under static and dynamic walking were shown in Fig. 19 and 20 for proximal and distal part respectively and under static and dynamic stair-climbing were shown in Fig. 21 and 22 for proximal and distal part respectively.

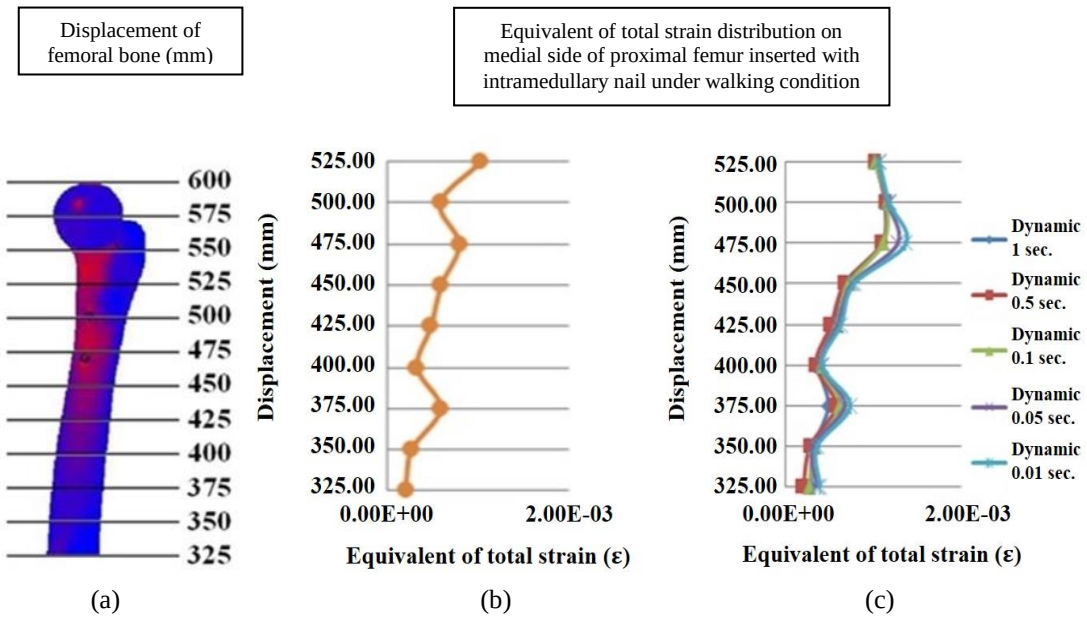

Fig. 19. Equivalent of total strain distribution at medial side of proximal femur inserted with intramedullary nail: (a) Femoral bone, (b) Static loading condition and (c) Dynamic loading condition.

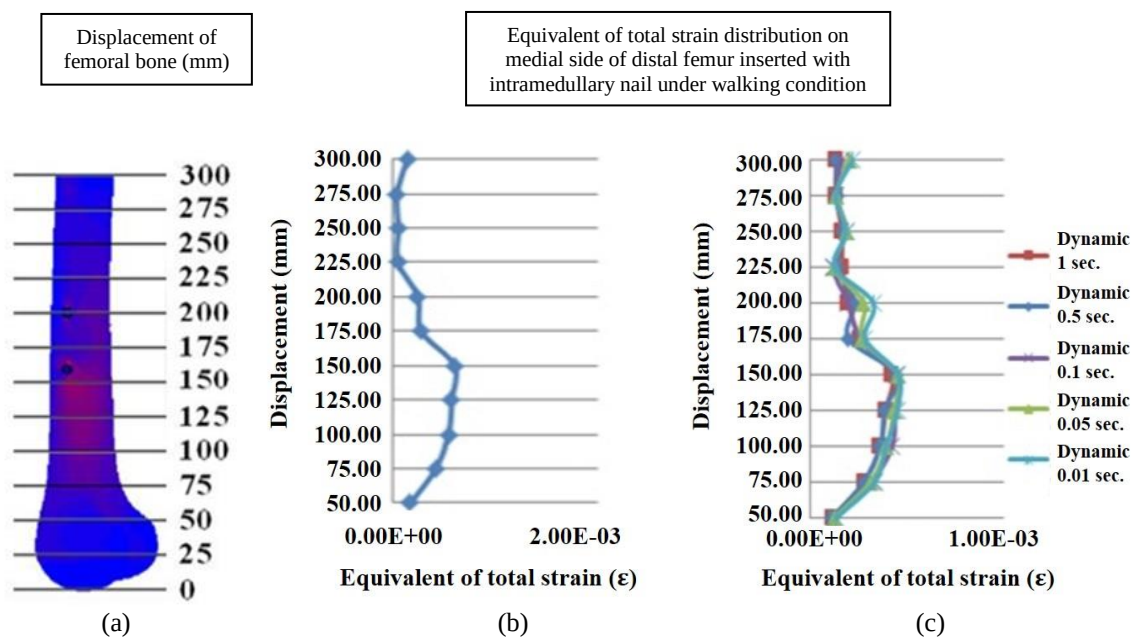

Fig. 20. Equivalent of total strain distribution at medial side of distal femur inserted with intramedullary nail: (a) Femoral bone, (b) Static loading condition and (c) Dynamic loading condition.

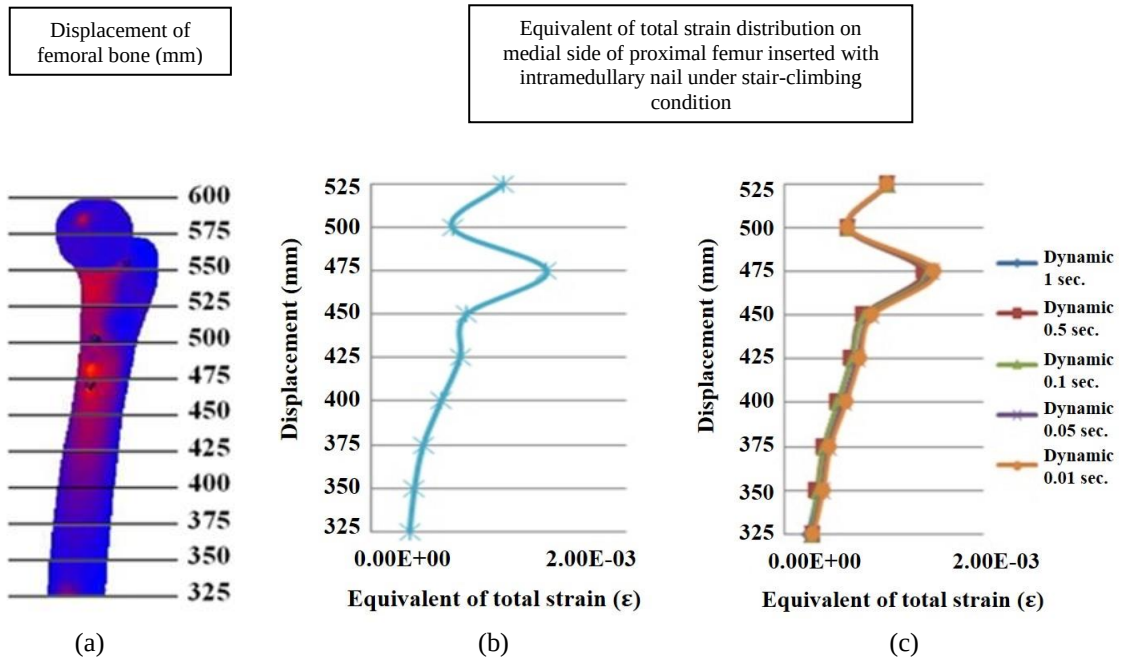

Fig. 21. Equivalent of total strain distribution at medial side of proximal femur inserted with intramedullary nail: (a) Femoral bone, (b) Static loading condition and (c) Dynamic loading condition.

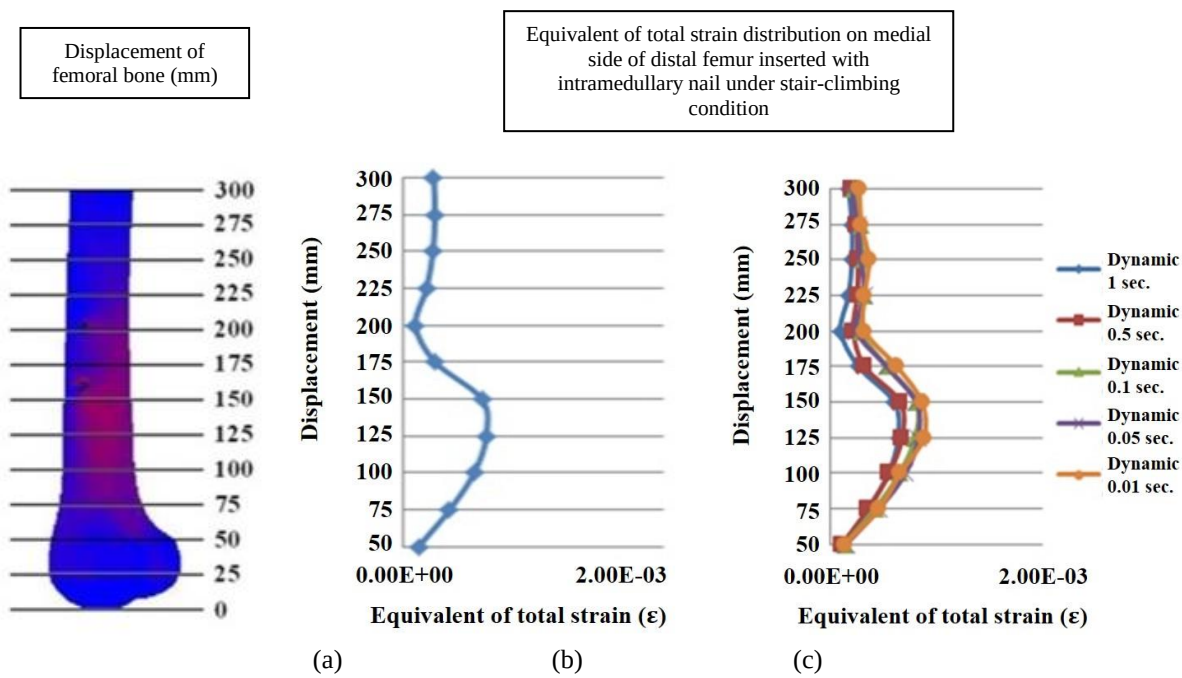

Fig. 22. Equivalent of total strain distribution at medial side of distal femur inserted with intramedullary nail: (a) Femoral bone, (b) Static loading condition and (c) Dynamic loading condition.

The maximum equivalent of total strain on femoral bone of all models did not exceed 25,000 με; and the trend of the maximum equivalent of total strain distribution when varied time under dynamic loading condition was shown in Fig. 23 and 24 under walking and stair-climbing respectively.

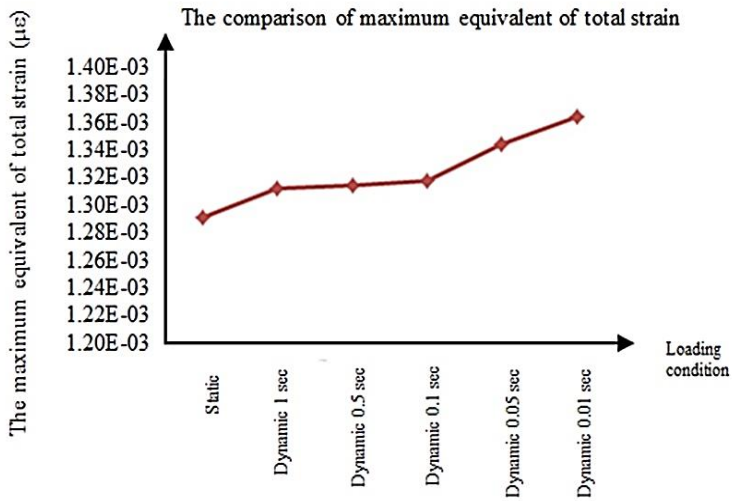

Fig. 23. The comparison of the maximum equivalent of total strain on femur inserted with intramedullary nail at the medial side under static walking and dynamic walking varied time condition.

The comparison of maximum equivalent of total strain on femoral bone between static and dynamic condition had 9.52% difference in case of 1 sec gait cycle, 10.68% in case of 0.5 sec gait cycle, 11.65% in case of 0.1 sec gait cycle, 23.30% in case of 0.05 sec gait cycle and 29.47% in case of 0.01 sec gait cycle under walking condition and 1.10% in case of 1 sec gait cycle, 1.23% in case of 0.5 sec gait cycle, 5.34% in case of 0.1 sec gait cycle, 7.19% in case of 0.05 sec gait cycle and 9.35% in case of 0.01 sec gait cycle under stair-climbing condition. When the time of gait cycle decreased, the maximum strain distribution on the bone increased; it showed that the strain distribution varies inversely with time of gait cycle.

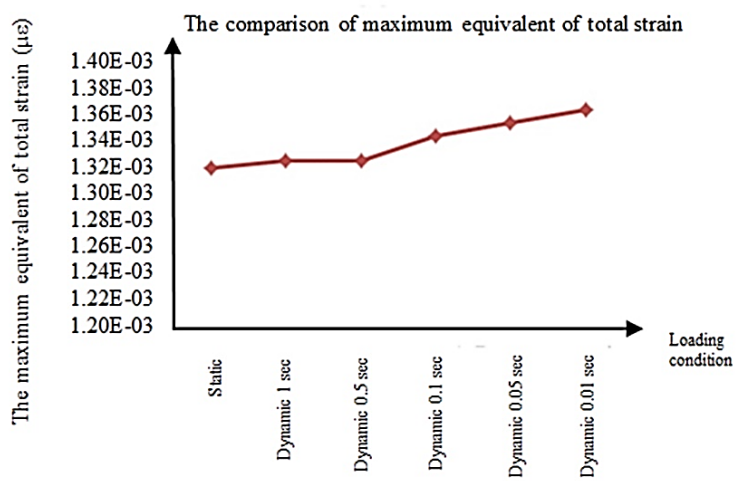

Fig. 24. The comparison of the maximum equivalent of total strain on femur inserted with intramedullary nail at the medial side under static stair-climbing and dynamic stair-climbing varied time condition.

3.4 Fracture fragment

The equivalent of total strain of the fracture fragment of bone inserted with intramedullary nail was evaluated in twelve cases as static walking, static stair-climbing, dynamic walking 1, 0.5, 0.1, 0.05 and 0.01 second and dynamic stair-climbing 1, 0.5, 0.1, 0.05 and 0.01 second. The maximum equivalent of total strain in each case was shown in Table 4.

Table 4: The maximum equivalent of total strain on fracture fragment under walking and stair-climbing condition.

Condition	The maximum of equivalent of total strain (με)	
	Walking	Stair-climbing
Static	151,553	180,034
Dynamic 1 second	219,071	226,618
Dynamic 0.5 second	253,995	263,233
Dynamic 0.1 second	272,761	283,413
Dynamic 0.05 second	281,174	291,394
Dynamic 0.01 second	329,251	331,608

The trend of the maximum equivalent of total strain distribution when varied time under dynamic loading were shown in Fig. 25 and 26 under walking and stair-climbing respectively.

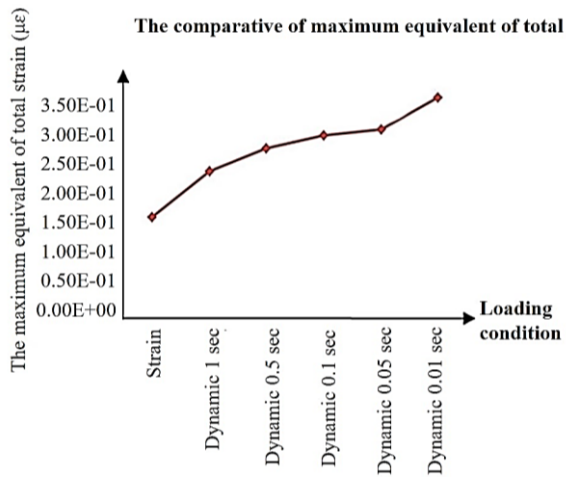

Fig. 25. The comparison of the maximum equivalent of total strain on fracture fragment under static walking and dynamic walking varied time condition.

The fracture fragment had maximum equivalent of total strain over 150,000 microstrain under all conditions. Therefore, the bone remodeling by natural healing mechanisms is slightly slower because, in the natural healing process, the maximum equivalent total strain should not exceed 4,000 microstrain for a good result. The bone healing with intramedullary nail should not bear the full load until the end of the healing process.

The static and dynamic loading conditions on the maximum equivalent of total strain on femur and femur inserted with hip prosthesis shared nearly similar results because load-bearing devices were absolutely fixed to the femur. On the other hand, the static and dynamic loading conditions on the maximum equivalent of total strain femur inserted with intramedullary nail showed great difference because load-sharing devices had a micro-motion that accumulated energy that can only be captured by dynamic loading condition. This study focused on the material properties of bone under elastic deformation and did not analyzed the fatigue condition on femur.

3.5 Hip prosthesis

The maximum von Mises stress of hip prosthesis was evaluated under static walking, static stair-climbing, dynamic walking and dynamic stair-climbing condition. The maximum von Mises stress in each case was shown in Table 5 and the stress distribution on hip prosthesis under static walking was shown in Fig. 25.

Table 5: The maximum von Mises stress on hip prosthesis under walking and stair-climbing condition.

Condition	Maximum von Mises stress (MPa)	
	Walking	Stair-climbing
Static	311.6	312.2
Dynamic 1 second	311.6	312.2
Dynamic 0.5 second	312.9	313.6
Dynamic 0.1 second	314.3	315.8
Dynamic 0.05 second	315.7	317.7
Dynamic 0.01 second	317.8	318.2

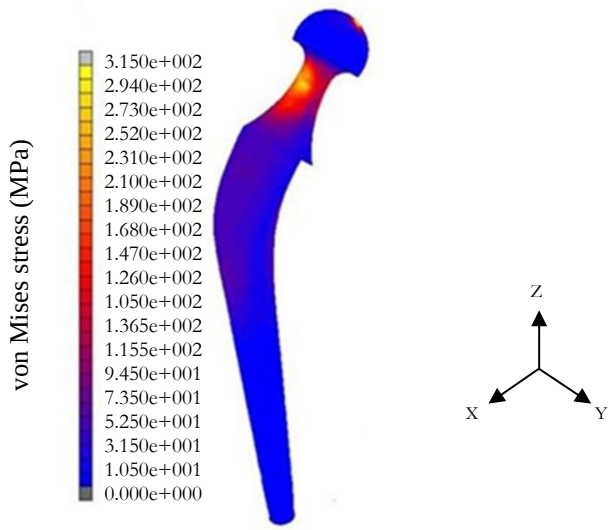

Fig. 25. The stress distribution on hip prosthesis under static walking condition.

The maximum von Mises stress on the prosthesis's model did not exceed the yield strength of titanium alloy [22]. The static and dynamic loading conditions showed slight difference in the maximum von Mises stress on the load-bearing devices because the hip prosthesis carried the load for the bone and the hip stem fit in the medullary canal. The maximum difference of von Mises stress between static and dynamic loading was 2.12%.

3.6 Intramedullary nail

The maximum von Mises stress of intramedullary nail was evaluated under static walking, static stair-climbing, dynamic walking and dynamic stair-climbing condition. The maximum von Mises stress in each case was shown in Table 6 and the stress distribution on intramedullary nail under static walking was shown in Fig. 26.

Table 6: The maximum von Mises stress on intramedullary nail under walking and stair-climbing condition.

Condition	Maximum von Mises stress (MPa)	
	Walking	Stair-climbing
Static	749.90	795.48
Dynamic 1 second	807.74	811.73
Dynamic 0.5 second	865.70	874.40
Dynamic 0.1 second	929.30	1,123.71
Dynamic 0.05 second	1,101.18	1,285.35
Dynamic 0.01 second	1,115.55	1,539.42

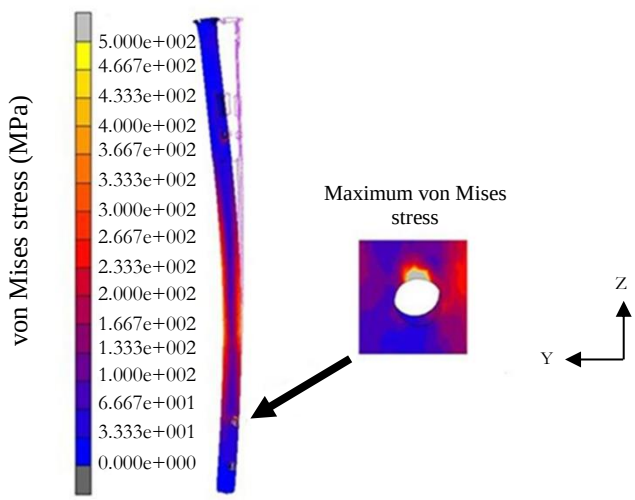

Fig. 26. The stress distribution on intramedullary nail under dynamic stair-climbing 0.01 second condition.

The fracture fragment cannot receive the load transfer from the proximal femur. The proximal part, thus, subsided and the upper distal screw hole received the load, making the maximum stress occur around the hole. The maximum von Mises stress on the intramedullary nail model exceeded the yield strength of stainless steel [22] in case of dynamic 0.1, 0.05 and 0.01 second. The maximum difference of von Mises stress between static and dynamic loading was 105.28%.

4. CONCLUSION

This research studied different results of static and dynamic loading conditions used to analyzed the femoral bone, load-bearing device and load-sharing device using finite element analysis. The static loading used the peak load of dynamic condition to act on the proximal femur but the dynamic loading was a continuous load, yielding different results in analysis.

4.1 Femoral bone

The static and dynamic loading conditions on the maximum equivalent of total strain on the femur inserted with intramedullary nail showed great difference, resulting in the equivalent of total strain on the fracture fragment exceeding 4,000 microstrain. Thus, the strain was in the overload zone of bone healing process on the model [20, 21]. The difference percentage of maximum equivalent of total strain between static and dynamic loading conditions was 118. Thus, dynamic loading condition is considered more suitable to analyze the load-sharing device case.

4.2 The implant

In case of load-bearing device, the static and dynamic loading conditions showed nearly similar value of stress distribution on the implant, with the percentage difference of maximum von Mises stress below 3. In case of load-sharing device, the static and dynamic loading conditions showed great difference of stress distribution on the implant, with the percentage difference of maximum von Mises stress over 105.

5. ACKNOWLEDGEMENT

The author wish to thank the Faculty of Medicine, Burapha University, Faculty of Engineering, Mahidol University, Thailand and Biomechanics Analysis and Orthopaedic Device Design Laboratory (B-AODD Lab) for their support with the facilities.

REFERENCES

[1] Aroonjarattham, P., Aroonjarattham K. and Suvanjumrat, C. Effect of mechanical axis on strain distribution after total knee replacement, J. Kasetsart (Nat. Sci.)., Vol. 48(2), 2014, pp. 263-282.

[2] Aroonjarattham, P., Aroonjarattham K. and Chanasakulniyom, M. Biomechanical effect of filled biomaterials on distal Thai femur by finite element analysis, J. Kasetsart (Nat. Sci.)., Vol. 49(2), 2015, pp. 263-276.

[3] Somtua, C., Aroonjarattham, P. and Aroonjarattham, K. The comparison of strain distribution on Thai normal, varus and total knee arthroplasty inserted femoral bone, Journal of Research and Applications in Mechanical Engineering, Vol. 2(1), 2014, pp. 42-50.

[4] Aroonjarattham, P., Aroonjarattham, K. and Somtua, C. The notch effect on strain distribution on Thai femoral bone after total knee arthroplasty, Journal of Research and Applications in Mechanical Engineering, Vol. 2(1), 2014, pp. 51-56.

[5] Heller, M.O., Bergman, G., Kassi, J.P., Claes, L., Hass, N.P. and Duda, G.N. Determination of muscle loading at the hip joint for use in pre-clinical testing, Journal of Biomechanics, Vol. 38(5), 2005, pp. 1155-1163.

[6] Gautier, E., Perren, S.M. and Ganz, R. Principle of internal fixation, Curr Orthop., Vol. 6(4), 1992, pp. 220-232.

[7] Bottner, F., Zawadsky, M., Su, E.P., Bostrom, M., Palm, L., Ryd, L., et al. Implant migration after early weightbearing in cementless hip replacement, Clin Orthop Relat Res., Vol. 436, 2005, pp. 132-137.

[8] Thomas, H.M., Adolph, V.L., Joseph, R.L., Hiroshi, F., Jodi, F.H., Suan, G.C., et al. Minimal 10-year results of a tapered cementless femoral component in total hip arthroplasty, J. Arthroplasty., Vol. 16(8 Suppl 1), 2001, pp. 49-54.

[9] Zalzal, P., Cheung, G., Bhandari, M., Spelt, J.K. and Papini, M. The load sharing characteristics and stress concentrations of a locked, retrograde, intramedullary femoral nail, Orthopaedic Proceeding, Vol. 90-B (supp I), 2008, pp. 71.
[10] Dowdy, P.A., Rorabeck, C.H. and Bourne, R.B. Uncemented total hip arthroplasty in patients 50 years of age or younger, J. Arthroplasty., Vol. 12(8), 1997, pp. 853-862.
[11] Mallory, T.H., Head, W.C. and Lombardi, A.V. Tapered design for the cementless total hip arthroplasty femoral component, Clin Orthop Relat Res., Vol. 344, 1997, pp. 172-178.
[12] Hellman, E.J., Capello, W.N. and Feinberg, J.R. Omnifit cementless total hip arthroplasty: a 10-year average follow-up, Clin Orthop Relat Res., Vol. 364, 1999, pp.164-174.
[13] Head, W.C., Mallory, T.H. and Emerson Jr, R.H. The proximal porous coating alternative for primary total hip arthroplasty, Orthopedics, Vol. 22(9), 1999, pp. 813-815.
[14] Stephenson, P. and Seedhom, B.B. Cross-section geometry of the human femur in the mid-third region., Proc Inst Mech Eng H., Vol. 213(2), 1999, pp. 159-66.
[15] Zalzal, P., Backstein, D., Gross, A.E. and Papini, M. Notching of the anterior femoral cortex during total knee arthroplasty, J. Arthroplasty., Vol. 21(5), 2006, pp. 737-743.
[16] Bregmann, G. HIP98, 2001, Free University, Berlin.
[17] Senalpati, S.K. and Pal, S. Uhmwpe-alumina ceramic composite, an improved prosthesis material for an artificial cement hip joint, Trends Biomater Artif Organs., Vol. 16, 2002, pp. 5-7.
[18] Peraz, C., Mahar, A., Negus, C., Newton, P. and Impelluso, T. A computational evaluation of the effect of intramedullary nail material properties on the stabilization of simulated femoral shaft fracture, Med Eng Phys., Vol.30(6), 2007, pp. 755-760.
[19] Ramos, A. and Simoes, J.A. Tetrahedral versus hexahedral finite elements in numerical modeling of the proximal femur, Med Eng Phy., Vol. 28, 2006, pp. 916-924.
[20] Frost, H.M. Wolff's law and bone's structural adaptation to mechanical usage: an overview for clinicians, The Angle Orthodontist, Vol. 64(3), 1994, pp. 175-188.
[21] Frost, H.M. Update of bone physiology and wolff's law for clinicians, Angle Orthodontist, Vol. 74, 2003, pp. 3-15.
[22] Black, J. and Hastings. G. Handbook of biomaterials properties, 1998, Chapman & Hall, UK.